Evidence of Charge Multiplication in Thin $25\mu m \times 25\mu m$ Pitch 3D Silicon Sensors

A. Gentry[1], M. Boscardin[2,3], M. Hoeferkamp[1], M. Povoli[4], S. Seidel[1], J. Si[1], G.-F. Dalla Betta[3,5]

[1]Department of Physics and Astronomy, University of New Mexico, [2]Fondazione Bruno Kessler,[3]TIFPA INFN,[4]SINTEF Digital,[5]Department of Industrial Engineering, Università degli Studi di Trento and INFN

Second DRD3 Workshop on Solid State Detector R&D
December 2, 2024

Motivation

- 3D sensors were first used in ATLAS's Insertible B Layer (IBL) a decade ago, with $250\mu m \times 50\mu m$ layout, designed to withstand $5 \times 10^{15} \mathrm{n_{eq}/cm^2}$
- Smaller geometries are planned to be used soon in the innermost layers of ATLAS's and CMS's upgraded trackers, with layouts $25\mu m \times 100\mu m$ and $50\mu m \times 50\mu m$ [1, 2, 3]
- However, both experiments plan for removal of the inner layers in the mid-2030's due to the extreme radiation at the High Luminosity LHC (HL-LHC) [4]
- There is interest in implementing rad-hard detectors with both excellent spatial and timing resolution (4D tracking) at that stage in the barrel region, to complement the timing information of the planned forward-region disk timing layers [5, 6]
- Already, $50\mu m \times 50\mu m$ 3D sensors have been shown to have timing resolution better than $\sim$50 ps [7]
- Rad-hard 4D tracking will be essential at potential future hadron colliders, where an order of magnitude larger radiation dose and pileup are expected [8, 9, 10]

$5\times10^{15}\mathrm{n_{eq}/cm^2}$

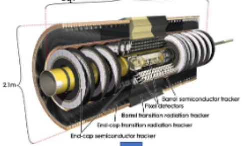

$2\times10^{16}\mathrm{n_{eq}/cm^2}$

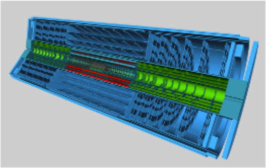

$8\times10^{17}\mathrm{n_{eq}/cm^2}$

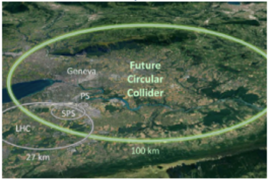

$25\mu\text{m} \times 25\mu\text{m}$ 3D Sensors

- A set of $25\mu\text{m} \times 25\mu\text{m}$ 3D sensors has been designed at the University of Trento and fabricated at Fondazione Bruno Kessler (FBK)
- Simulations made previously have indicated that sensors with this column pitch could have timing resolution in the realm of $\sigma_t = 13$ ps[7, 5]
- Simulations have indicated that a very tight geometry could lead to large enough electric fields along the column length to cause impact ionization charge multiplication below the breakdown voltage
- This can be controlled, i.e. multiplication not at the column tip or detector surface, which would be much less predictable

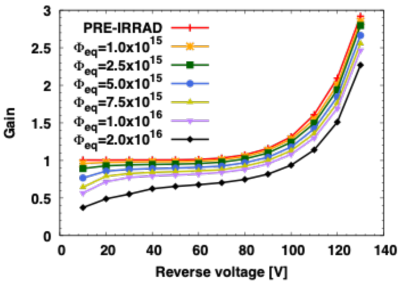

Figure taken from: Marco Povoli et al. "Feasibility Study of Charge Multiplication by Design in Thin Silicon 3D Sensors". In: *IEEE Nuclear Science Symposium.* 2019, N30-02

$25\mu m \times 25\mu m$ 3D Sensors

- Sensors with $25\mu m \times 25\mu m$ and $50\mu m \times 50\mu m$ pitch with otherwise identical designs have been characterized at UNM
- Fabricated with step-and-repeat (stepper) lithography at FBK, allowing for nominal 150 μm active thickness and very small pitch
- p-type substrate bonded to a 500μm thick low-resistivity support wafer, device processed from front side
- Due to boron diffusion, actual active thickness is $\sim 140\mu m$
- p-type columns are etched, penetrating to the support wafer, allowing the sensor to be biased from the back side
- n-type columns are etched, with $\sim 35\mu m$ gap between column tip and support wafer to prevent early breakdown
- Column width is $\sim 5\mu m$
- Prototypes are 20×20 arrays of pixels with electrodes connected with aluminum to a bond pad

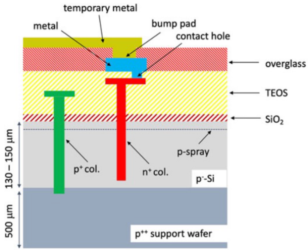

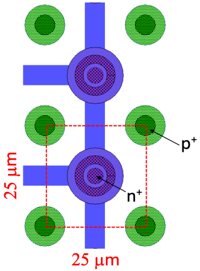

I-V and C-V Measurements

- I-V and C-V measurements made by placing sensor in a dark box on a Peltier-cooled chuck at 20°C
- Biased from the back side with Keithley 237, measured through a probe on the bond pad
- Temperature scaled to $-45°$C, to match temp used for later measurements, using equation: [11]

$$I(T_2) = I(T_1) \times \left(\frac{T_2}{T_1}\right)^2 \exp\left(\frac{E_{\text{eff}}}{2k_B}\left(\frac{1}{T_2} - \frac{1}{T_1}\right)\right). \quad (1)$$

- Typical leakage current below 1 nA, when scaled to $-45°$C at 80V, and breakdown in the range 60-120V at $+20°$C

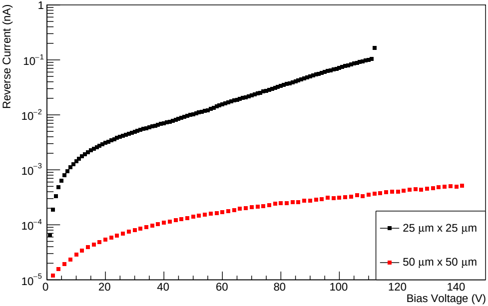

I-V and C-V Measurements

- CV measurements use HP4284A LCR meter and bias isolation box to measure capacitance
- Depletion voltage in the range 2-4 V; necessary to over-deplete due to radial electric field
- Typical capacitance at 10 V is ∼ 22 pF

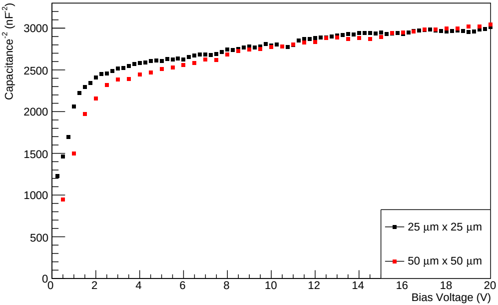

Charge Collection Setup

- Custom readout PCB with low noise was designed at UNM
- Sensors connected to copper pad with conductive tape; sensor is biased from pad
- 2 stages of GALI-S66+ monolithic Darlington pair amplifiers are used
  - GALI-S66+ has bandwidth DC-3GHz, ~ 20 dB gain and noise figure 2.4 dB
- Electronic components are covered by EMI shields, one covering and isolating each stage of amplification, and covering the components on the back side of the PCB
- Output is further amplified by Particulars AM-02B amplifier
- Noise filtered by Crystek CLPFL-1000 1 GHz low-pass filter

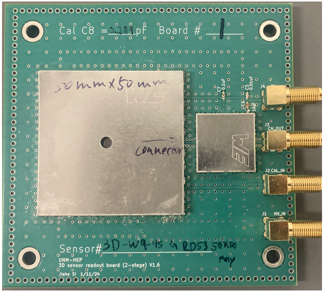

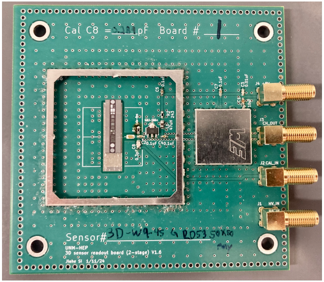

Charge Collection Setup

- Signals are read out by Tektronix DPO7254 2.5 GHz 40 GS/s oscilloscope (20 GS/s w/ 2 channels)
- ^{90}Sr MIP's are used for coincidence measurements with an LGAD detector with excellent S/N as the reference, and 3D DUT below
- Devices placed in a thermal chamber at $-45°$C to reduce noise
- Read out waveforms are integrated in software between points where voltage crosses 0, to calculate charge

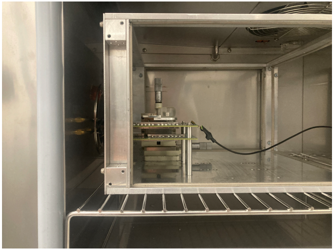

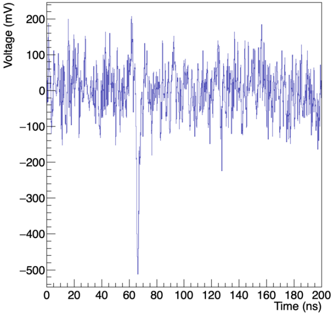

Charge Calibration

- Calibration input uses a capacitor pulsed by a function generator
- Calibration carried out with multiple different capacitances as a cross-check and for error quantification
- Pulses read out identically, 1000 waveforms are collected at a range of input voltages
- Resulting charge histograms are fit with a Gaussian
- Gaussian mean vs. input voltage is fit with a line; the slope gives the conversion factor to standard units of charge
- Estimated 3.5% uncertainty in calibration

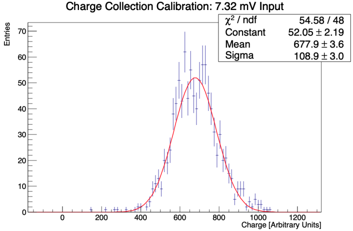

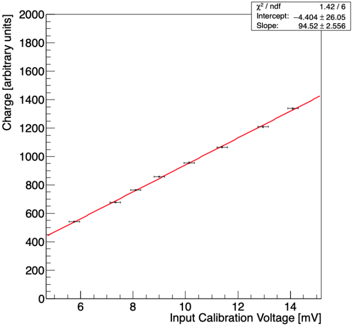

Charge Fit

- 10,000 waveforms were collected at a range of bias voltages below breakdown
- To characterize noise, data were collected without the beta source first
- This distribution was fit with a Gaussian times a sigmoid function - the sigmoid accounts for the cutoff due to the trigger threshold
- Then the data with the source is fit with the Gaussian×sigmoid plus a Landau convolved with a Gaussian
- The fit parameters from the pure noise fit are constrained in the fit to the data with the source

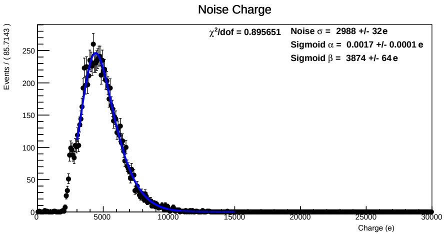

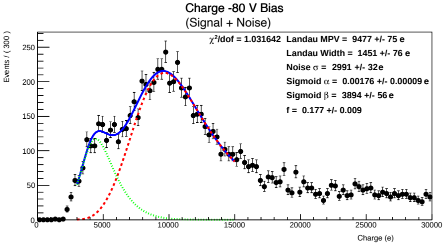

Most Probable Value (MPV) vs. Bias Voltage

- Charge Landau MPV vs. bias voltage, with comparison between an example $25\mu\mathrm{m} \times 25\mu\mathrm{m}$ sensor and $50\mu\mathrm{m} \times 50\mu\mathrm{m}$ sensor
- The typical charge collection for the $25\mu\mathrm{m} \times 25\mu\mathrm{m}$ array between 10-80V is about 9400 e^-, which is consistent with the expectation of 67 e-h pairs per $\mu\mathrm{m}$ for 140 $\mu\mathrm{m}$ active thickness
- Gain starts at about 90V bias consistently across $25\mu\mathrm{m} \times 25\mu\mathrm{m}$ arrays
- No gain up to breakdown for $50\mu\mathrm{m} \times 50\mu\mathrm{m}$ observed or predicted
- Maximum gain below breakdown is 1.33

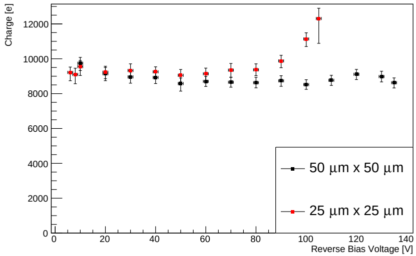

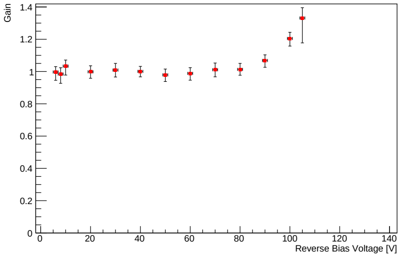

Error Analysis

- Statistical error in charge collection measurements is quantified by dividing the 10,000 waveforms into subsets and fitting each subset
  - Statistical error is the standard deviation of the MPV's divided by the square root of the number of subsets
- One source of systematic error is the choice of the convolution Gaussian σ, which is fixed in the fit
  - It is not well constrained in the fit, due to the cutoff of the upper tail of the Landau due to the maximum voltage of the oscilloscope
  - In a wide range, from about 100 to 1000e^-, the χ^2/dof changes $<$10%
  - The value of the constant σ was varied in increments of 50 e^- and the best fit value was used
  - the range for which the χ^2/dof is within 10% of the best value is taken as the error range for this systematic effect
- The oscilloscope trigger threshold can also be a source of systematic error
  - The threshold was varied and data collected at the same bias voltage, after accounting for variation due to statistical error, 3% error is attributed to the trigger threshold
- Error bars on the plots in the previous slide show these 3 error sources added in quadrature, but not the calibration error

Conclusions

- 3D sensors with $25\mu\mathrm{m} \times 25\mu\mathrm{m}$ pitch were developed. Characterizations of these sensors have been carried out, including I-V, C-V and charge collection measurements
- These devices are expected to have excellent radiation hardness due to the extremely small interelectrode separation, and could have excellent timing resolution
- Charge collection results show gain below breakdown for multiple devices, with gain factor up to 1.33
- A subset of these detectors has been irradiated at LANL and Sandia, and work characterizing these is ongoing
- The result, which is consistent with simulation predictions of gain, demonstrates the feasibility of implementing charge multiplication by-design in 3D sensors, opening up a number of possibilities for further improving the technology
- This work is available at arXiv:2409.03909-physics.ins-det
- Accepted to JINST 11/12/24

Acknowledgments

This work is supported by the U.S. Department of Energy, the National Science Foundation, and the New Mexico Space Grant Consortium (NASA)

References I

[1] M. Capeans et al. "ATLAS Insertable B-Layer Technical Design Report". In: *CERN-LHCC-2010-013* (Sept. 2010) (cit. on p. 2).

[2] "Technical Design Report for the ATLAS Inner Tracker Pixel Detector". In: *CERN-LHCC-2017-021* (2017) (cit. on p. 2).

[3] "CMS Technical Design Report for the Pixel Detector Upgrade". In: *CERN-LHCC-2012-016* (Sept. 2012) (cit. on p. 2).

[4] Laura Gonella. "The ATLAS ITk detector system for the Phase-II LHC upgrade". In: *Nucl. Instrum. Meth. A* 1045 (2023), p. 167597 (cit. on p. 2).

[5] Gregor Kramberger. "Silicon detectors for precision track timing". In: *PoS* Pixel2022 (2023), p. 010 (cit. on pp. 2, 3).

[6] "Investigating the impact of 4D Tracking in ATLAS Beyond Run 4". In: *ATL-PHYS-PUB-2023-023* (2023) (cit. on p. 2).

[7] G. Kramberger et al. "Timing performance of small cell 3D silicon detectors". In: *Nucl. Instrum. Meth. A* 934 (2019), pp. 26–32 (cit. on pp. 2, 3).

References II

[8] A. Abada et al. "FCC-ee: The Lepton Collider: Future Circular Collider Conceptual Design Report Volume 2". In: *Eur. Phys. J. Spec. Top.* 228.2 (2019), pp. 261–623 (cit. on p. 2).

[9] A. Abada et al. "FCC-hh: The Hadron Collider: Future Circular Collider Conceptual Design Report Volume 3". In: *Eur. Phys. J. Spec. Top.* 228.4 (2019), pp. 755–1107 (cit. on p. 2).

[10] M. I. Besana et al. "Evaluation of the radiation field in the future circular collider detector". In: *Phys. Rev. Accel. Beams* 19.11 (2016), p. 111004 (cit. on p. 2).

[11] Alexander Chilingarov. "Temperature dependence of the current generated in Si bulk". In: *JINST* 8.10 (2013), P10003 (cit. on p. 5).